

MMA Memo 223: Yet Another Look at Anomalous Refraction

M.A. Holdaway
National Radio Astronomy Observatory
and
David Woody
Owens Valley Radio Observatory

July 22, 1998

Abstract

The previous treatments of anomalous refraction by Holdaway (MMA Memo 186) and by Butler (MMA Memo 188) were in error in two ways. First, they only accounted for one dimension of anomalous refractive pointing. For the zenith case, this increases the pointing error by $\sqrt{2}$. Second, the assumed elevation dependence of the phase structure function was incorrect. Working from Holdaway and Ishiguro (MMA Memo 127), both Holdaway and Butler assumed that the phase structure function, calculated with the physical baseline, varies directly with airmass. Reevaluating the situation indicates that the phase structure function must be calculated with the projected baseline. The result is a less pronounced increase of anomalous refractive pointing jitter with airmass. Finally, because the phase structure function must be calculated with the projected baseline, we have incorrectly transferred the phase structure function from the phase monitor system to the zenith (and to all other elevations as well). The net effect of these three errors is an increase in the anomalous refractive pointing jitter of about 25-50% for most observations over the values reported by Holdaway and by Butler. We still find a weak dependence of anomalous refractive pointing on the dish diameter. Further, we indicate how the anomalous refraction might be considered in antenna design.

1 Anomalous Refractive Pointing in Two Dimensions

Both Holdaway and Butler failed to include the effect of the azimuthal phase fluctuations in their treatment of anomalous refraction. For isotropic turbulence, the azimuth and elevation contributions will be the same at the zenith, so the total zenith refractive pointing jitter needs to increase by $\sqrt{2}$. However, the treatment made by Holdaway and by Butler would indicate that at low elevations, the pointing errors in the elevation direction will be larger than the pointing errors in the azimuth direction by a factor of

$$(\sec z)^\alpha,$$

where z is the zenith angle and α is root phase structure function exponent defined by

$$\sigma_\phi(\rho) = \sqrt{D_\phi(\rho)} \simeq A\rho^\alpha,$$

ρ being the baseline. There has been no observed difference in the refractive pointing jitter in the azimuth and elevation directions.

2 Phase Structure Function: Physical or Projected Baseline?

The difference between the azimuth and elevation components of the refractive pointing jitter are due to the assumption made by both Holdaway and Butler that the relevant baseline to calculate the phase structure on is $d \sec z$, where d is the dish diameter. This is equivalent to saying that the phase structure function must be calculated with the physical baselines of an interferometer. On the other hand, if the phase structure function must be calculated with the projected baselines of an interferometer, and the dish samples the phase structure function on an unprojected baseline of d , then the azimuth and elevation components of the refractive pointing jitter will be equal.

Figure 1 shows rms phase as a function of physical baseline. The data were taken with the VLA at 22 GHz on June 6, 1997 in CnB array over a 2 hour period looking at a single source about transit with a mean elevation angle of 39 degrees. We thank Chris Carilli for the use of his data. The reported phases are the rms over the full 2 hour period after removing a quadratic trend. In order to increase the signal to noise of these phase observations, we solved for the antenna based phases and differenced them on each baseline to determine the baseline phase. This results in an increase in SNR of about 3.6. We neglected IF 1 due to instrumental phase instabilities, but IF 2 showed excellent instrumental phase stability. Only on the very shortest baselines below 100 m do we start to see any indications of instrumental noise contributing to the atmospheric phase fluctuations.

The most striking thing about Figure 1 is that it shows *two* structure functions, one for predominately east-west baselines, represented by open squares, and one for predominately north-south baselines, represented by filled squares. Since our source was transiting, the N-S baselines were all projected, but the E-W baselines were not. When we replot the data again using the projected baseline in Figure 2, we find that the scatter decreases markedly.

However, if the phase structure function must be calculated using the projected baseline, does it therefore follow that the results of Holdaway and Ishiguro (1995), which used the physical baseline, imply a steeper elevation dependence of the phase structure function? The data from Holdaway and Ishiguro have also been reanalyzed using the projected baseline rather than the physical baseline. Because that data were taken in three subarrays rather than with the entire array, there are not enough visibilities to state clearly that the projected baseline gives less scatter than the physical baseline. A global statistical analysis revealed that on the 0-400 m baseline range, the phase structure function varies like airmass raised to the 0.90 power when the physical baselines are used, but like airmass raised to the 1.06 power when the

projected baselines are used. Neither exponent differs significantly from the theoretical value of 1.0.

Hence, the phase structure function is proportional to the airmass when the projected baseline is used. Not only does this change the form of the equation for the anomalous refraction pointing error (given below), but it also has implications for any scaling of the phase structure function to spatial scales different than the 300 m (206 m in projection) baseline which is measured with the site testing interferometer. For the median α of 0.6, the rms phase on some projected baseline will be about $(300/206)^{0.6} = 1.25$ times larger than previously quoted values. This correction increases the magnitude of the anomalous refraction for all telescope diameters.

Furthermore, this also applies to the analysis of the success of fast switching phase calibration. The old fast switching analysis indicated that the distance between the lines of sight, as measured in the plane of the atmosphere, could become very large at low elevation angles, leading to large residual phase errors. However, the correct quantity to calculate is the phase structure function evaluated at the projected distance between the lines of sight, which is much smaller at low elevation angles. Hence, fast switching will work somewhat better than we thought.

Everything we have stated above deals with baselines or effective baselines which are assumed small compared to the thickness of the turbulent layer. The expectation is that for turbulent layers much thicker than the physical baseline, you are in the 3-D turbulence regime and the structure function for the projected baseline should be applicable. For long baselines where the turbulent layer is much thinner than the projected baseline, you are in the 2-D turbulence regime and the structure function for the physical baseline should be used. Anomalous refraction for single telescopes and fast switching phase calibration on 10 s time scales will always be in the 3-D turbulence regime.

3 Back to Anomalous Refraction

Accumulating the above corrections, we believe the correct expression for the rms anomalous refraction pointing error, in radians, is

$$\sigma_p(d, z) = \frac{\sqrt{2D_l(d) \sec z}}{d},$$

or as a fraction of the beam width:

$$\sigma_p(d, z) = \frac{\sqrt{2D_l(d) \sec z}}{\lambda}.$$

On Chajnantor, the root phase structure function typically increases as the baseline raised to the 0.6 power, so the refractive pointing as a fraction of the beam will increase with the dish diameter raised to the 0.6 power.

Using these expressions, we calculate the refractive pointing jitter for the first, second, and third quartile phase stability conditions at Chajnantor, and for 8, 10, 12, and 15 m dish diameter in Table 1.

1st Quartile Refractive Pointing Jitter elevation					
$d[\text{m}]$	90°	50°	30°	20°	10°
8	0.48 (0.48)	0.55 (0.55)	0.69 (0.69)	0.83 (0.83)	1.17 (1.17)
10	0.44 (0.55)	0.51 (0.63)	0.63 (0.79)	0.76 (0.96)	1.07 (1.34)
12	0.42 (0.63)	0.48 (0.72)	0.59 (0.89)	0.70 (1.06)	1.00 (1.49)
15	0.38 (0.72)	0.44 (0.82)	0.54 (1.00)	0.65 (1.21)	0.92 (1.72)
2nd Quartile Refractive Pointing Jitter elevation					
$d[\text{m}]$	90°	50°	30°	20°	10°
8	0.93 (0.93)	1.06 (1.06)	1.31 (1.31)	1.58 (1.58)	2.23 (2.23)
10	0.85 (1.06)	0.97 (1.21)	1.20 (1.49)	1.45 (1.82)	2.04 (2.55)
12	0.79 (1.18)	0.90 (1.35)	1.11 (1.66)	1.35 (2.03)	1.90 (2.85)
15	0.72 (1.35)	0.83 (1.57)	1.03 (1.93)	1.24 (2.33)	1.75 (3.27)
3rd Quartile Refractive Pointing Jitter elevation					
$d[\text{m}]$	90°	50°	30°	20°	10°
8	1.96 (1.96)	2.24 (2.24)	2.78 (2.78)	3.36 (3.36)	4.72 (4.72)
10	1.79 (2.24)	2.04 (2.55)	2.54 (3.17)	3.06 (3.82)	4.30 (5.37)
12	1.68 (2.52)	1.92 (2.88)	2.37 (3.55)	2.86 (4.29)	4.02 (6.02)
15	1.54 (2.88)	1.75 (3.27)	2.16 (4.05)	2.62 (4.92)	3.68 (6.89)

Table 1: Pointing jitter caused by anomalous refraction for 8, 10, 12, and 15 m dishes at observing elevations of 90, 50, 30, 20, and 10 degrees. Values in parentheses are in terms of the fraction of the 1/30 beamwidth pointing error specification.

Table 2: Image dynamic range and fidelity index for four different simple pointing error types, each of magnitude 2 arcseconds (8m dishes, 345 GHz observing frequency). *Global* is a constant pointing offset shared by all antennas, *drift* is a linear pointing drift shared by all antennas, *random 1* is random among antennas but constant in time, while *random 2* is random in both antennas and time.

Pointing Error Type	Dynamic Range	Image Fidelity
Global	83	8.05
Drift	149	12.88
Random 1	398	24.72
Random 2	805	37.39

4 Estimation of Limiting Mosaicing Quality

The MMA Advisory Committee (MAC) has recommended that the anomalous refraction pointing errors be excluded from the antenna specifications. While the anomalous refraction is not a major driver in the antenna specifications, it needs to be considered, and we wish to demonstrate a reasonable approach here.

Table 2 shows the effects of pointing errors on the image dynamic range and fidelity, based on mosaic simulations with different kinds of pointing errors (reproduced from MMA Memo 178). Refractive pointing jitter will be most closely approximated by “Random 2” type pointing errors, which are the most benign. The dynamic range scales like $1/\theta_{PE}$, so for the case of an 8m dish observing at a 50 degree elevation, the median anomalous refraction will be 1.06 arcseconds, and the limiting image dynamic range will be 1770:1. For 10m: 1520:1. For 12m: 1360:1. For 15m: 1180:1. Now, realistic pointing errors will include some more systematic terms, which will actually limit the dynamic range to something worse than these numbers. However, there is at least the possibility of performing some sort of pointing error self-cal on these more systematic pointing errors. There is little chance of performing the pointing self-cal on the anomalous refraction pointing errors, since they are both random in time and among antennas. This means that we need to have very high signal to noise in each ~ 1 s integration. There will be many observing conditions in which anomalous refraction could limit the mosaic dynamic range of bright objects.

References

- Butler, Bryan, 1997, MMA Memo 188: “Another look at anomalous refraction on Chajnantor”.
- Holdaway, M.A., and Ishiguro, M., 1995, MMA Memo 127: “Experimental Determination of the Dependence of Tropospheric Pathlength Variation on Airmass”.

Holdaway. M.A., 1997, MMA Memo 186: "Calculation of Anomalous Refraction on Chajnantor".

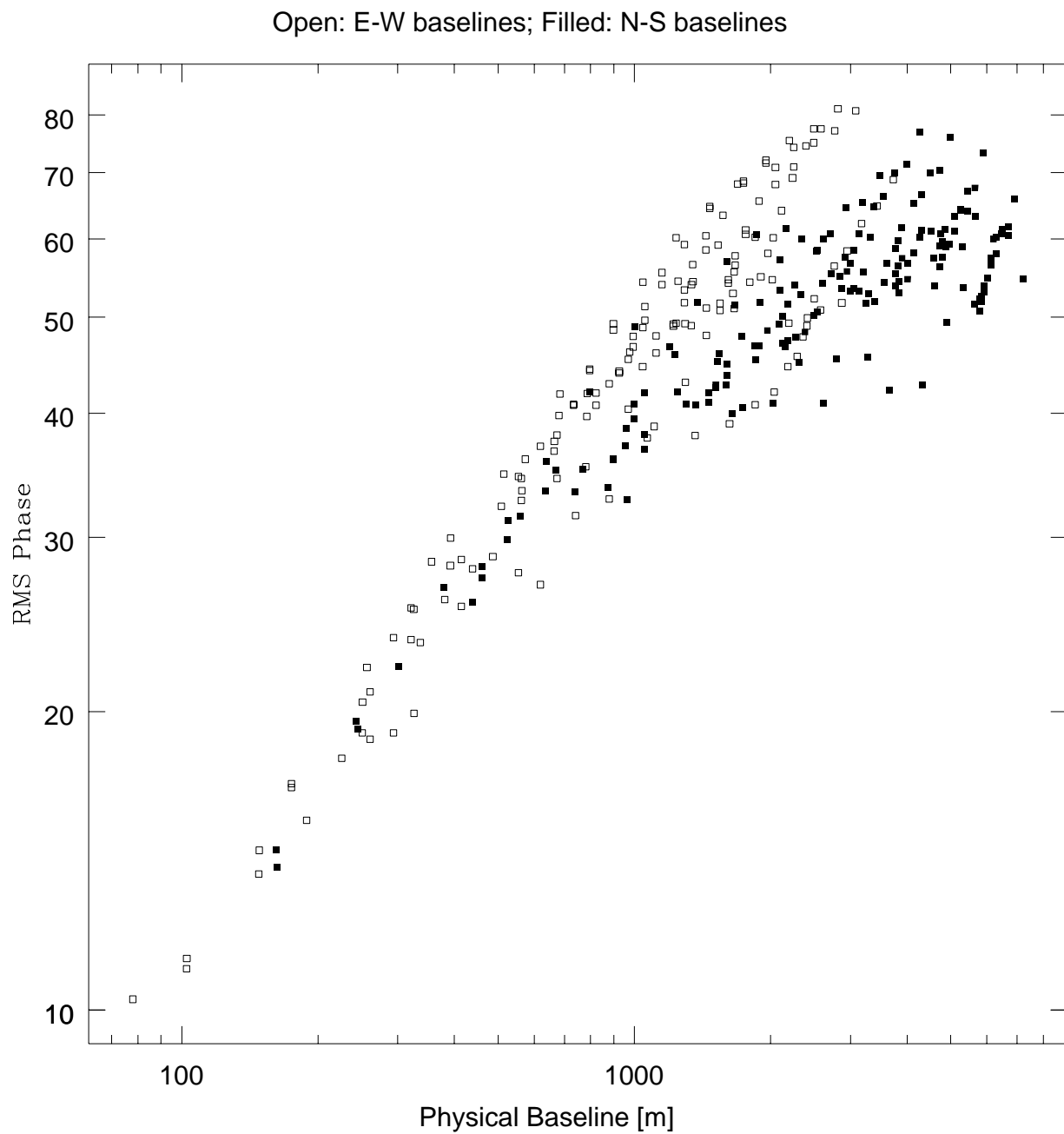


Figure 1: Root phase structure function from VLA data using the *physical* baselines. Note the wide scatter between the N-S and E-W baselines.

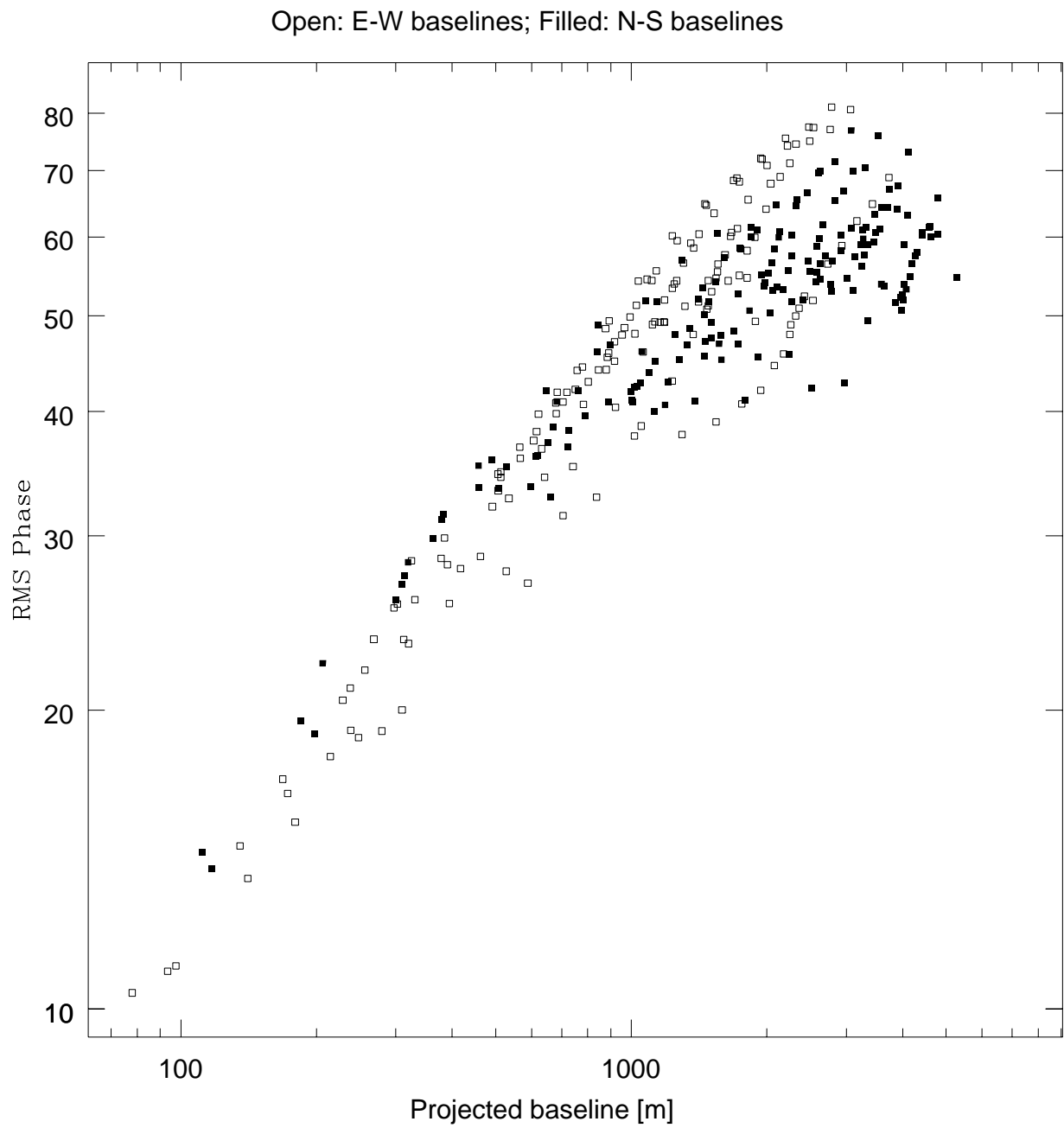


Figure 2: Root phase structure function from VLA data using the *projected* baselines. Much of the scatter between the N-S and E-W baselines goes away.

Median Refractive Pointing (10m): (0.7 1.4 2.8 5.6 arcs)

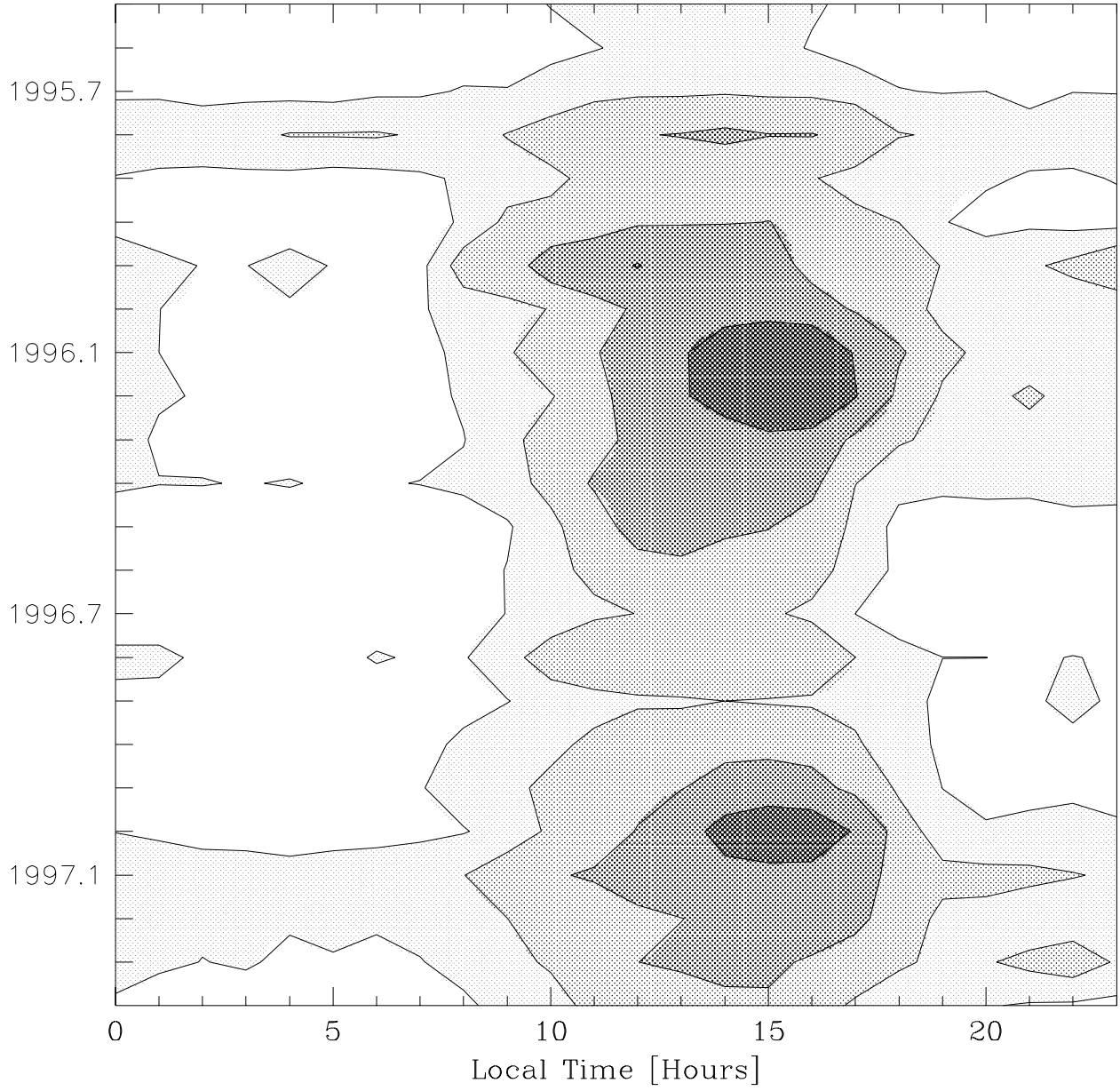


Figure 3: Contours of the median pointing error caused by refractive jitter on the Chajnantor site as a function of time of day and month of the year.